



ELSEVIER

Contents lists available at SciVerse ScienceDirect

Organic Electronics

journal homepage: www.elsevier.com/locate/orgel

Letter

Tandem photovoltaic cells based on low-concentration donor doped C₆₀Minlu Zhang^a, Hui Wang^b, C.W. Tang^{a,b,*}^a Department of Chemical Engineering, University of Rochester, Rochester, NY 14627, United States^b Department of Physics and Astronomy, University of Rochester, Rochester, NY 14627, United States

ARTICLE INFO

Article history:

Received 3 October 2011

Received in revised form 14 November 2011

Accepted 15 November 2011

Available online 27 November 2011

Keywords:

Tandem photovoltaic cell

Bulk heterojunction

Low-concentration donor

C₆₀

ABSTRACT

We demonstrate that enhanced efficiency can be achieved in organic tandem photovoltaic cells using identical bulk heterojunction subcells based on 1,1-bis-(4-bis(4-methyl-phenyl)-amino-phenyl)-cyclohexane doped C₆₀ in series. Power conversion efficiencies greater than 4% have been achieved in 2- and 3-stack tandem cells, an improvement of at least 30% over the single-stack cell.

© 2011 Published by Elsevier B.V.

The power conversion efficiency of organic photovoltaic (OPV) cells has been improved significantly by optimizing the design of various bulk heterojunction (BHJ) structures [1–4]. For most OPV cells, the power conversion efficiency (PCE) is often limited by light absorption due to the use of thin BHJ layers and mismatch between the BHJ absorption and the solar spectrum [5]. A method to increase the cell efficiency is to use a tandem cell architecture. In a series-connected tandem cell, two or more subcells with complementary absorption spectra are generally used to improve the overall absorption and to provide a matched photocurrent from individual subcells [5–10]. Subcells with identical compositions have also been used as tandem structure; however, the efficiency enhancement is generally marginal [11–13]. In this paper, we show that enhanced efficiency can be obtained in tandem cells based on identical subcells [14] where C₆₀ is the sole absorber.

The single-stack cell structure is as follows: ITO/MoO_x/BHJ/bathophenanthroline (Bphen)/Al. The 2- and 3-stack tandem cells are composed of the subcells connected serially by an inter-connecting layer (ICL). The schematic 2-stack tandem cell structure is shown in Fig. 1. The BHJ

layer is a mixed film of 1,1-bis-(4-bis(4-methyl-phenyl)-amino-phenyl)-cyclohexane (TAPC) doped in C₆₀ layer. The concentration of TAPC in the BHJ layer is 5% (by volume) for all the cells in this paper. Except for the thickness of BHJ layer, the thickness of all the other layers is kept constant: ITO (90 nm), MoO_x (2 nm), Bphen (8 nm for single-stack cell; 6 nm for tandem subcell) and Al (100 nm). The ICL consists of a layer of Ag (0.3 nm) [15] and a layer of 1,4,5,8,9,11-hexaazatriphenylene hexacarbonitrile (HAT-CN) (1.5 nm) [16]. The substrate is a patterned ITO glass obtained from a commercial source. The fabrication process is as follows: the substrate was cleaned and subjected to oxygen plasma prior to loading into a custom-built vacuum chamber for thin film deposition [17]. All the organic materials for thin film deposition were purified by entrainer gas sublimation before use [18,19]. Thin film deposition was carried out in the vacuum chamber where the entire layer sequence, including the deposition of the MoO_x anode buffer layer and the top Al electrode, were completed at a pressure of 6×10^{-7} Torr without a vacuum break. The deposition rates, in Å/s, for MoO_x, TAPC, C₆₀, Bphen, Ag, HAT-CN and Al are typically 2, 0.1, 1.9, 2, 0.3, 2 and 6, respectively. For the TAPC-doped C₆₀ layer, the volume ratio of the donor to C₆₀ was controlled by independently varying the rate of deposition of the two components using an Inficon IC5 controller. The cell active

* Corresponding author at: Department of Chemical Engineering, University of Rochester, Rochester, NY 14627, United States.

E-mail address: ching.tang@rochester.edu (C.W. Tang).

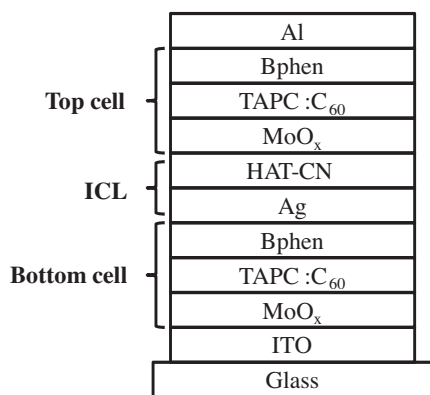


Fig. 1. Schematic layer structure of the 2-stack tandem cell.

area, 0.1 cm^2 , was defined by the overlapping area of the ITO and Al electrodes. An Oriel 150 W Xe lamp with an AM 1.5G filter was used to provide an intensity of 100 mW/cm^2 for illumination. The light intensity was determined by a Si diode (with KG-5 visible color filter, Hamamatsu S1787-04) calibrated by NREL. Spectral mismatch has not been taken into account for our power efficiency measurement. Current–voltage curves were obtained with a Keithley model 2400 source meter.

Fig. 2 shows the variation of the open-circuit voltage (V_{oc}), short-circuit current density (J_{sc}), fill factor (FF) and PCE versus the BHJ layer thickness for a single-stack cell. Each data point represents the average of four current

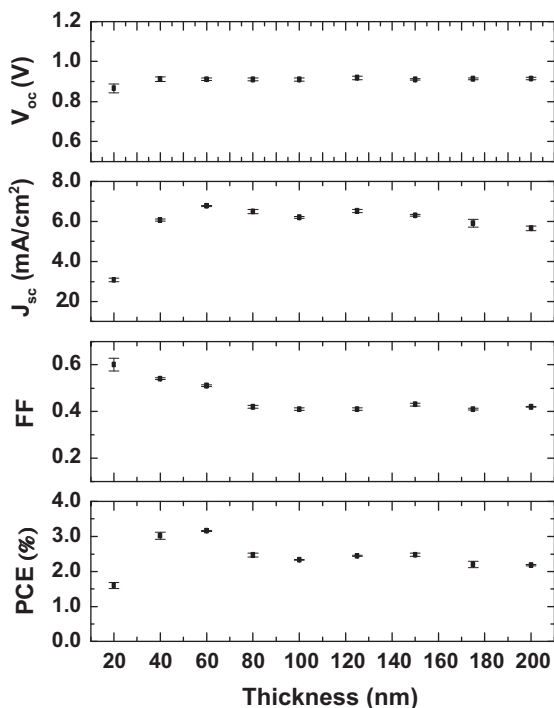


Fig. 2. Photovoltaic characteristics of TAPC:C₆₀ single-stack cells with various BHJ layer thickness.

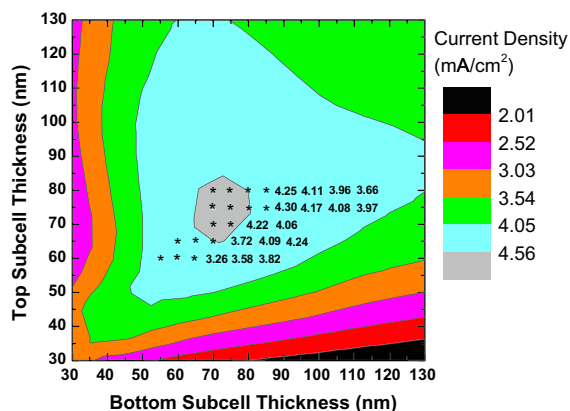


Fig. 3. Contour plot of simulated current density of 2-stack tandem cells. Star points are the experimental results with the current density indicated accordingly.

density–voltage (J – V) measurements. Several features are noteworthy: (1) the V_{oc} ($\sim 0.9 \text{ V}$) is independent of the BHJ layer thickness; (2) the J_{sc} increases with the BHJ layer thickness up to 60 nm, beyond which it shows a small but noticeable oscillatory behavior; (3) the FF decreases from a maximum of 0.6 to a minimum of 0.4 beyond 80 nm; (4) the best photovoltaic performance (PCE $\approx 3\%$) is obtained with the BHJ thickness in the range of 40–60 nm. At this thickness the cell only absorbs less than 60% of photons in the C₆₀ absorption region. Further increasing the BHJ layer thickness only results in a large decrease in the FF without any enhancement in J_{sc} . To solve this issue, a tandem structure cell is used.

To optimize the thickness of subcells in the tandem cells, we apply the device model [20] that we have used in our previous paper for the single-stack cells [14]. Photon absorption is calculated using an optical transfer-matrix theory [21,22], and the exciton dissociation is described

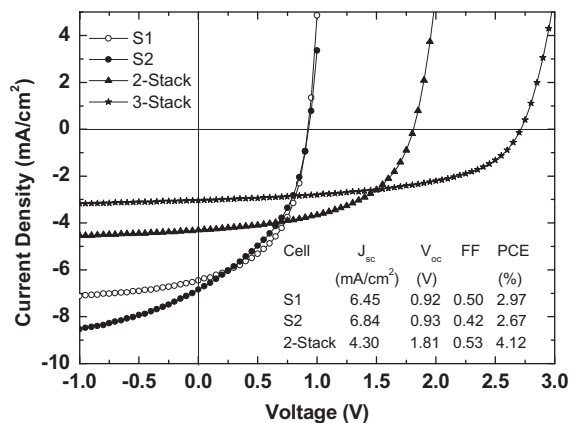


Fig. 4. Current density–voltage characteristics of two single-stack cells: S1 (70 nm) and S2 (145 nm); a 2-stack tandem cell composed of a bottom subcell (70 nm) and a top subcell (75 nm); and a 3-stack tandem cell composed of a bottom subcell (50 nm), a middle subcell (85 nm) and a top subcell (70 nm). The inset shows the summary of the cell performance.

Table 1Optimized photovoltaic performance of TAPC:C₆₀ single-stack cell, 2-stack and 3-stack tandem cells.

| Cell | BHJ layer thickness (nm) | V _{oc} (V) | J _{sc} (mA/cm ²) | FF | PCE (%) |
|--------------|--------------------------|---------------------|---------------------------------------|------|---------|
| Single-stack | 60 | 0.91 | 6.77 | 0.51 | 3.14 |
| 2-Stack | 70/75 | 1.81 | 4.30 | 0.53 | 4.12 |
| 3-Stack | 50/85/70 | 2.71 | 3.08 | 0.53 | 4.42 |

by the Braun–Onsager model [23,24]. We also assume that the ICL acts as a recombination center in the tandem cell. The simulation parameters we used here were reported in our previous papers [14,25], except that the built-in potential is doubled ($V_{bi} = 1.81$ V) for the tandem cell. Fig. 3 shows the contour plot of simulated current density for the combinations of bottom and top subcells with various BHJ layer thicknesses. The maximum current density region is shown where the thickness of both subcells is around 70 nm. To confirm the simulated results, a series of tandem cells with bottom and top subcells thicknesses of around that range were constructed. The experimental data of tandem cells are shown as the start points with the values indicated accordingly, which quite match the simulated results. Based on the simulation, an optimized tandem cell with improved power conversion efficiency was fabricated.

Fig. 4 shows the J - V characteristics of two single-stack cells, S1 and S2, and a 2-stack tandem cell. The BHJ layer thickness of S1 and S2 cells is 70 and 145 nm, respectively. The 2-stack tandem cell consists of a bottom subcell (70 nm) and a top subcell (75 nm). The performance of these cells is summarized in the inset of Fig. 4. For the cell S1, the J_{sc} is approximately saturated due to the nearly field-independent charge generation. In contrast, the J_{sc} of cell S2, which has a thicker BHJ layer, is not saturated. The increase in photocurrent at reverse bias is due to increased absorption of the BHJ layer and a field-dependent photogeneration efficiency. In addition, the FF in the cell S2 drops to 0.42, resulting in an overall reduction in cell efficiency. For the 2-stack tandem cell, the V_{oc} is nearly doubled compared with the single-stack cells, whereas the J_{sc} is reduced by less than 40%. Furthermore, a high FF of 0.53 is retained, indicating the photogeneration in the tandem subcells is relatively field-independent, similar to the cell S1. The slightly improved FF can be attributed to a redistribution of the built-in electric field in the subcells as a result of the required current matching in the subcells [26]. The gain in V_{oc} , which is more than offset the reduction of J_{sc} , has resulted in an overall improvement in efficiency (4.12%).

To further improve the power conversion efficiency of TAPC:C₆₀ cell, we fabricated 3-stack cells with bottom, middle, and top subcells connected by Ag/HAT-CN. The highest PCE for the 3-stack tandem cell was obtained using BHJ of 50, 85, and 70 nm, respectively, for the subcells. These thicknesses were based on the simulation which was also used for the 2-stack tandem cell. The J - V characteristic of the 3-stack tandem cell was shown in Fig. 4. The optimized photovoltaic performances for this 3-stack cell are summarized in Table 1 along with the single-stack and 2-stack cells. Due to the measurement without using an aperture mask, the efficiency we reported here could be overestimated by 2%. In comparison, the improved

performances of tandem cells are derived from: (1) the V_{oc} is almost exactly multiplied according to the number of stacks; (2) the J_{sc} is reduced, but less than expected; (3) the FF is slightly improved. The overall power conversion efficiencies are improved by 31% and 41% for the 2-stack and 3-stack tandem cells, respectively.

In conclusion, we have demonstrated enhanced performance in organic tandem cells with identical subcells consisting of TAPC doped C₆₀. Power conversion efficiencies greater than 4% have been achieved in 2-stack and 3-stack tandem cells with optimized BHJ thickness and composition.

References

- [1] S.H. Park, A. Roy, S. Beaupre, S. Cho, N. Coates, J.S. Moon, D. Moses, M. Leclerc, K. Lee, A.J. Heeger, *Nat. Photonics* 3 (2009) 297–302.
- [2] W.L. Ma, C.Y. Yang, X. Gong, K. Lee, A.J. Heeger, *Adv. Funct. Mater.* 15 (2005) 1617–1622.
- [3] G. Li, V. Shrotriya, J.S. Huang, Y. Yao, T. Moriarty, K. Emery, Y. Yang, *Nat. Mater.* 4 (2005) 864–868.
- [4] Y.Y. Liang, Z. Xu, J.B. Xia, S.T. Tsai, Y. Wu, G. Li, C. Ray, L.P. Yu, *Adv. Mater.* 22 (2010) E135–E138.
- [5] A. Hadipour, B. de Boer, P.W.M. Blom, *Adv. Funct. Mater.* 18 (2008) 169–181.
- [6] J. Yang, R. Zhu, Z.R. Hong, Y.J. He, A. Kumar, Y.F. Li, Y. Yang, *Adv. Mater.* 23 (2011) 3465–3470.
- [7] M. Riede, C. Uhrich, J. Widmer, R. Timmreck, D. Wynands, G. Schwartz, W.M. Gnehr, D. Hildebrandt, A. Weiss, J. Hwang, S. Sundarraj, P. Erk, M. Pfeiffer, K. Leo, *Adv. Funct. Mater.* 21 (2011) 3019–3028.
- [8] D. Cheyns, B.P. Rand, P. Heremans, *Appl. Phys. Lett.* 97 (2010) 033301.
- [9] S. Sista, Z.R. Hong, L.M. Chen, Y. Yang, *Energy Environ. Sci.* 4 (2011) 1606–1620.
- [10] T. Ameri, G. Dennler, C. Lungenschmied, C.J. Brabec, *Energy Environ. Sci.* 2 (2009) 347–363.
- [11] R. Timmreck, S. Olthof, K. Leo, M.K. Riede, *J. Appl. Phys.* 108 (2010) 033108.
- [12] X.W. Sun, D.W. Zhao, L. Ke, A.K.K. Kyaw, G.Q. Lo, D.L. Kwong, *Appl. Phys. Lett.* 97 (2010) 053303.
- [13] D.J.D. Moet, P. de Bruyn, J.D. Kotlarski, P.W.M. Blom, *Org. Electron.* 11 (2010) 1821–1827.
- [14] M. Zhang, H. Wang, H. Tian, Y. Geng, C.W. Tang, *Adv. Mater.* 23 (2011) 4960–4964.
- [15] J.G. Xue, S. Uchida, B.P. Rand, S.R. Forrest, *Appl. Phys. Lett.* 85 (2004) 5757–5759.
- [16] L.S. Liao, W.K. Slusarek, T.K. Hatwar, M.L. Ricks, D.L. Comfort, *Adv. Mater.* 20 (2008) 324–329.
- [17] M. Zhang, Irfan, H.J. Ding, Y.L. Gao, C.W. Tang, *Appl. Phys. Lett.* 96 (2010) 183301.
- [18] K. Sakai, M. Hiramoto, *Mol. Cryst. Liq. Cryst.* 491 (2008) 284–289.
- [19] R.A. Laudise, C. Kloc, P.G. Simpkins, T. Siegrist, *J. Cryst. Growth* 187 (1998) 449–454.
- [20] L.J.A. Koster, E.C.P. Smits, V.D. Mihailetchi, P.W.M. Blom, *Phys. Rev. B* 72 (2005) 085205.
- [21] L.A.A. Pettersson, L.S. Roman, O. Inganas, *J. Appl. Phys.* 86 (1999) 487–496.
- [22] N.K. Persson, H. Arwin, O. Inganas, *J. Appl. Phys.* 97 (2005) 034503.
- [23] L. Onsager, *J. Chem. Phys.* 2 (1934) 599–615.
- [24] C.L. Braun, *J. Chem. Phys.* 80 (1984) 4157–4161.
- [25] M. Zhang, H. Wang, C.W. Tang, *Appl. Phys. Lett.* 97 (2010) 143503.
- [26] A. Hadipour, B. de Boer, P.W.M. Blom, *Org. Electron.* 9 (2008) 617–624.